Title	Finite element based generalized impedance boundary condition for complicated em calculation
Author(s)	He, S; Nie, Z; Huang, JZ; Jiang, L; Chew, WC
Citation	The 2011 IEEE International Symposium on Antennas and Propagation (APSURSI), Spokane, WA., 3-8 July 2011. In IEEE APSURSI Digest, 2011, p. 2700-2703
Issued Date	2011
URL	http://hdl.handle.net/10722/140269
Rights	Creative Commons: Attribution 3.0 Hong Kong License

Finite Element Based Generalized Impedance Boundary Condition for Complicated EM Calculation

Shiquan He, Zaiping Nie
School of Electronic Engineering
University of Electronic Science and Technology of China
Chengdu, China
shiquanhe@uestc.edu.cn, zpnie@uestc.edu.cn

Jun Zh. Huang, Lijun Jiang*, Weng Cho Chew
Department of Electrical and Electronic Engineering
University of Hong Kong
Hong Kong, HKSAR, China
huangjun@eee.hku.hk, jianglj@hku.hk, wcchew@hku.hk

***Abstract*—In this paper, a finite element based generalized impedance boundary condition (FEM-GIBC) is proposed to solve complicated electromagnetic (EM) problems. Complex structures with arbitrary inhomogeneity and shapes are modeled with the finite element method, and their scattering contributions are transformed to generalized impedance conditions on their boundaries. For each sub-domain, a special GIBC can be established and it is only related to the structures in this domain. Hence, for finite periodic structures, a representative GIBC can be formulated at the boundary of a unit cell. After the GIBC at each boundary is established, the electromagnetic coupling between each impedance boundary can be calculated by the boundary integral equations (BIE) and accelerated with the multilevel fast multipole algorithm (MLFMA).**

Keywords-finite element method; generalized impedance boundary condtion ; boundary integral equation

I. INTRODUCTION

In engineering applications, we usually need to analyze the electromagnetic (EM) effects of complicated structures or devices working in complex environments. Full-wave solvers governed by Maxwell's equations play critical roles in predicting their EM responses. Among various full-wave EM solvers, boundary integral equations (BIE) associated with the method of moments (MoM) or fast algorithms [1] have been extensively used to analyze perfect electric conductors (PEC) and homogeneous dielectrics for years because only surface discretization is needed and they satisfy the radiation boundary condition automatically. Surface discretization has the advantage that unknowns reside only on surfaces, which usually means a much smaller number of unknowns.

In order to preserve the superiority of boundary integral equation methods, some approximation methods, for example, the impedance boundary condition (IBC) [2], thin dielectric sheet (TDS) [3] approximation have been proposed to solve special cases for non-perfect conductors, thin dielectric structures or thin dielectric coatings. The IBC defines a simple local relation between the surface current and electric field so that it only introduces a trivial extra cost compared with PEC problems. However, it is a local planar approximation and validated upon rigorous effective conditions. Generally, a better accuracy can be achieved by changing the local relation to a global one on the whole boundary, namely, the generalized impedance boundary conditions (GIBC).

Supported by '111Project', China (No. B07046), and GRF grants: RGC, (No. 711508 and 711609), ITF (No. ITS/159/09), Hong Kong Government.

In our previous work [4], a GIBC derived from the PMCHWT like surface integral equations have been presented to accurately model conductors with finite conductivity. In this paper, a novel GIBC is derived from the finite element method (FEM) for arbitrary inhomogeneous media applications which are usually encountered in integrate circuit (IC) simulation and EM analysis with complex environment. The whole 3D space can be separated into several sub-domains by the geometry boundaries of embedded structures, or by some fictitious surfaces. At each boundary, a GIBC can be established by utilizing the finite element method in the interior of each domain. It is only determined by the structures in this domain. Therefore, we actually have constructed a domain decomposition method (DDM) based on these generalized impedance boundary conditions. For finite periodic structures, the GIBC at each boundary has the same expression. Hence, a universal generalized impedance operator can be established at the boundary of a unit cell and the set up time of the final solution can be saved dramatically. Once the GIBC is established at each boundary, the coupling between them can be solved with conventional boundary integral equations and fast algorithms, such as multilevel fast multipole algorithm (MLFMA) can be used to accelerate the solution process.

II. BOUNDARY INTEGRAL EQUATION

As illustrated in Fig. 1(a), several inhomogeneous structures are embedded in a homogeneous background. Each inhomogeneous region and its boundary are represented by domain Ω_i and boundary S_i, $i=1, 2,..., N$, where N is the number of inhomogeneous regions. The homogenous background is defined as Ω_0. According to the equivalence principle [5], the EM field in Ω_0 can be generated by the radiation in a homogenous background from equivalent sources $\mathbf{J}_{si}$ and $\mathbf{M}_{si}$. $\mathbf{J}_{si}$ and $\mathbf{M}_{si}$ are located on S_i and expressed by $\mathbf{J}_{si} = \hat{n}_i \times \mathbf{H}_0$ and $\mathbf{M}_{si} = -\hat{n}_i \times \mathbf{E}_0$, as shown in Fig. 1(b). Here, $\mathbf{E}_0$ and $\mathbf{H}_0$ are the total field at Ω_0, and $\hat{n}_i$ denotes the outward unit normal vector.

Then, the total field can be expressed by

$$\mathbf{E}_0(\mathbf{r}) = \mathbf{E}_0^{inc}(\mathbf{r}) + \eta_0 \mathrm{L}\left(\sum_{i=1}^{N} \mathbf{J}_{si}\right) - \mathrm{K}\left(\sum_{i=1}^{N} \mathbf{M}_{si}\right) \quad (1)$$

$$\mathbf{H}_0(\mathbf{r}) = \mathbf{H}_0^{inc}(\mathbf{r}) + \frac{1}{\eta_0} \mathrm{L}\left(\sum_{i=1}^{N} \mathbf{M}_{si}\right) + \mathrm{K}\left(\sum_{i=1}^{N} \mathbf{J}_{si}\right) \quad (2)$$

Here, $\mathrm{L}(\bullet)$ and $\mathrm{K}(\bullet)$ are integral operators defined by (the time convention $e^{-i\omega t}$ is assumed)

$$\mathrm{L}(\mathbf{X}) = ik_0 \int_S \bar{\mathbf{G}}(\mathbf{r},\mathbf{r}') \bullet \mathbf{X}(\mathbf{r}') d\mathbf{r}', \quad \mathbf{r}' \in \bigcup S_i \tag{3}$$

$$\mathrm{K}(\mathbf{X}) = \int_S \nabla G(\mathbf{r},\mathbf{r}') \times \mathbf{X}(\mathbf{r}') d\mathbf{r}', \quad \mathbf{r}' \in \bigcup S_i \tag{4}$$

where $G(\mathbf{r},\mathbf{r}')$ and $\bar{\mathbf{G}}(\mathbf{r},\mathbf{r}')$ denote the scalar and dyadic Green's function in the homogeneous background, and k_0 and η_0 represent the wave number and wave impedance in the region Ω_0, respectively.

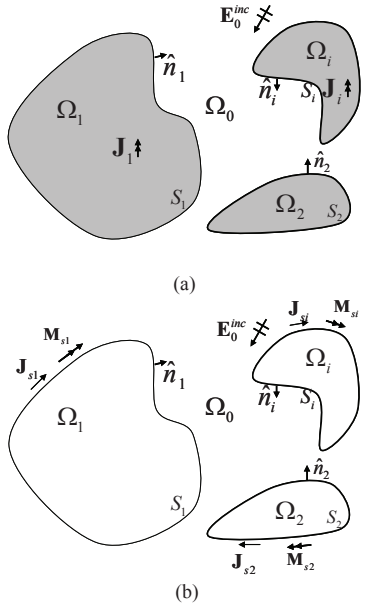

Figure 1. (a)A general problem involving multiple inhomogeneous regions. (b)Exterior equivalence for the initial problem.

According to the extinction theorem, four fundamental boundary integral equations-*TE, TH, NE* and *NH* formulations, can be established at each boundary S_i [6]. The *TE* formulation is listed as follows

$$\left[\mathbf{E}_0^{inc} + \eta_0 \mathrm{L}\left(\sum_{i=1}^{N} \mathbf{J}_{si} \right) - \mathrm{K}\left(\sum_{i=1}^{N} \mathbf{M}_{si} \right) \right]_{\tan} = 0, \quad \mathbf{r} \in S_i^- \tag{5}$$

where S_i^- denotes the inner side of boundary S_i (*i=1, 2, ...N*).

Equation (5) gives rise to a boundary integral equation with unknowns $\mathbf{J}_{si}$ and $\mathbf{M}_{si}$. To uniquely determine the values of $\mathbf{J}_{si}$ and $\mathbf{M}_{si}$, another boundary condition connecting the inner fields and boundary equivalent sources is required. If a GIBC is established as $\mathbf{M}_{si}(\mathbf{r}) = \mathrm{Z}_i(\mathbf{r},\mathbf{r}')\mathbf{J}_{si}(\mathbf{r}')$ ($\mathrm{Z}(\mathbf{r},\mathbf{r}')$ is defined as the generalized impedance operator. Integration is implied over repeated variables), it can be substituted into (5) to get a reduced equation only involving unknown $\mathbf{J}_{si}$. Consequently, equation (5) can be solved**.**

III. Finite Element Based Generalized Impedance Boundary Condition

The GIBC is derived from the PMCHWT like surface integral equation for homogeneous dielectric structures or conductors [4]. It also can be derived from the finite element method for arbitrary inhomogeneous applications [7].

A. Finite Element Discritization

The FEM solves the differential equation:

$$\nabla \times \bar{\mu}_{ri}^{-1} \bullet \nabla \times \mathbf{E}_i - k_0^2 \bar{\varepsilon}_{ri} \bullet \mathbf{E}_i = ik_0 \eta_0 \mathbf{J}_i \quad \mathbf{r} \in \Omega_i \tag{6}$$

$$\hat{n}_i \times \mathbf{E}_i = 0 \ \text{ on } S_i^{pec} \tag{7}$$

$$\hat{n}_i \times \mathbf{H}_i = \mathbf{J}_{si} \ \text{ on } S_i^{die} \tag{8}$$

where $\bar{\varepsilon}_{ri}$ and $\bar{\mu}_{ri}$ are the permittivity and the permeability in Ω_i, $\mathbf{J}_i$ represents the primary source in this region, and $\mathbf{E}_i$ and $\mathbf{H}_i$ are the electric and magnetic fields. S_i^{pec} is the PEC boundary. S_i^{die} denotes the dielectric interface. They construct the whole boundary S_i.

The finite element method converts the boundary value problem (6)-(8) to an optimization process

$$\begin{aligned} F(\mathbf{E}_i) = \frac{1}{2} \int_{\Omega_i} \left[(\nabla \times \mathbf{E}_i) \bullet \bar{\mu}_{ri}^{-1} \bullet (\nabla \times \mathbf{E}_i) - k_0^2 \mathbf{E}_i \bullet \bar{\varepsilon}_{ri} \bullet \mathbf{E}_i \right] dV \\ - ik_0 \eta_0 \int_{\Omega_i} \mathbf{E}_i \bullet \mathbf{J}_i dV + ik_0 \eta_0 \int_{S_i^{die}} \mathbf{E}_i \bullet \mathbf{J}_{si} dS \end{aligned} \tag{9}$$

The natural boundary condition (8) is embodied in the last term of (9), while the PEC boundary condition (7) needs to be constrained by decreasing the number of unknowns at the boundary. Sub-wavelength tetrahedrons and triangular patches are utilized to discretize the domain Ω_i and its boundary S_i, respectively. Then the inner electric field $\mathbf{E}_i$ and the boundary equivalent source $\mathbf{U}_i$ ($= ik_0 \eta_0 \mathbf{J}_{si}$) are represented by higher order finite-element basis functions [8] and the RWG basis functions [9]

$$\mathbf{E}_i = \sum_{j=1}^{N_i} e_{ij} \mathbf{N}_{ij} = \{\mathbf{N}_i\}^T \bullet \{e_i\} \tag{10}$$

$$\mathbf{U}_i = ik_0 \eta_0 \mathbf{J}_{si} = \sum_{j=1}^{L_i} u_{ij} \mathbf{S}_{ij} = \{\mathbf{S}_i\}^T \bullet \{u_i\} \tag{11}$$

where $\{\mathbf{N}_i\} = (\mathbf{N}_{i1}, \mathbf{N}_{i2}, ...\mathbf{N}_{iN_i})^T$, $\{S_i\} = (S_{i1}, S_{i2}, ...S_{iL_i})^T$, $\{e_i\} = (e_{i1}, e_{i2}, ...e_{iN_i})^T$, and $\{u_i\} = (u_{i1}, u_{i2}, ...u_{iL_i})^T$. Here, $\mathbf{N}_{ij}$ is the *j-th* finite element basis function in the domain Ω_i, $\mathbf{S}_{ij}$ is the *j-th* RWG basis function, and e_{ij} and u_{ij} denote the weights of each basis function. N_i and L_i are their numbers.

According to the variational principle, we can establish a linear equation about $\{e_i\}$ and $\{u_i\}$:

$$[K_i]\{e_i\} + [B_i]\{u_i\} = \{V_i\}. \tag{12}$$

Here, $[K_i]$ is the stiffness-mass matrix in FEM, $[B_i]$ is a boundary connection matrix, and $\{V_i\}$ is the excitation vector. Each element of them is calculated by

$$[K_i]_{mn} = \int_{\Omega_i} \left[(\nabla \times \mathbf{N}_{im}) \cdot \bar{\mu}_{ri}^{-1} \cdot (\nabla \times \mathbf{N}_{in}) - k_0^2 \mathbf{N}_{im} \cdot \bar{\varepsilon}_{ri} \cdot \mathbf{N}_{in} \right] dV \tag{13}$$

$$[B_i]_{mn} = \int_{S_i} \mathbf{N}_{im} \cdot \mathbf{S}_{in} dS \ \text{ i.e. } [B_i] = \{\mathbf{N}_i\} \bullet \{\mathbf{S}_i\}^T \tag{14}$$

$$\{V_i\}_j = ik_0 \eta_0 \int_{\Omega_i} \mathbf{N}_{ij} \cdot \mathbf{J}_i dV \ \text{ i.e. } \{V_i\} = ik_0 \eta_0 \{\mathbf{N}_i\} \bullet \mathbf{J}_i \tag{15}$$

Notice that (12) has given a connection between the boundary equivalent source $\mathbf{J}_{si}$ and the inner field $\mathbf{E}_i$ in a discretized form.

B. Generalized Impedance Boundary Condition

From (12), $\{e_i\}$ can be expressed as

$$\{e_i\} = [K_i]^{-1} \bullet \left(\{V_i\} - [B_i]\{u_i\} \right). \quad (16)$$

Hence,

$$\begin{aligned} \mathbf{E}_i &= \{\mathbf{N}_i\}^T \bullet \{e_i\} \\ &= \{\mathbf{N}_i\}^T \bullet [K_i]^{-1} \bullet \left(\{V_i\} - [B_i]\{u_i\} \right) \\ &= ik_0\eta_0 \{\mathbf{N}_i\}^T \bullet [K_i]^{-1} \bullet \{\mathbf{N}_i\} \bullet (\mathbf{J}_i - \mathbf{J}_{si}). \end{aligned} \quad (17)$$

There is a two-term summation in (17). The first term is called the incident field while the second term is the scattered field. They are represented as the following formats

$$\mathbf{E}_i^{inc}(\mathbf{r}) = ik_0\eta_0 \{\mathbf{N}_i\}^T \bullet [K_i]^{-1} \bullet \{\mathbf{N}_i\} \bullet \mathbf{J}_i(\mathbf{r}') \quad (18)$$

$$\mathbf{E}_i^{sca}(\mathbf{r}) = -ik_0\eta_0 \{\mathbf{N}_i\}^T \bullet [K_i]^{-1} \bullet \{\mathbf{N}_i\} \bullet \mathbf{J}_{si}(\mathbf{r}'). \quad (19)$$

According to the definition of $\mathbf{M}_{si}$, we have

$$\begin{aligned} \mathbf{M}_{si} &= -\hat{n}_i \times \mathbf{E}_i \\ &= -\hat{n}_i \times \left(ik_0\eta_0 \{\mathbf{N}_i\}^T \bullet [K_i]^{-1} \bullet \{\mathbf{N}_i\} \bullet (\mathbf{J}_i - \mathbf{J}_{si}) \right). \end{aligned} \quad (20)$$

The above has connected $\mathbf{M}_{si}$ with $\mathbf{J}_{si}$. Equation (20) is essentially the generalized impedance boundary condition. Therefore the generalized impedance operator is defined as

$$\mathrm{Z}_i(\mathbf{r}, \mathbf{r}') = ik_0\eta_0 \hat{n}_i \times \{\mathbf{N}_i\}^T \bullet [K_i]^{-1} \bullet \{\mathbf{N}_i\} \quad \text{when } \mathbf{J}_i = 0. \quad (21)$$

C. Matrix Solving

Similar to equation (11), we continue expressing $\mathbf{M}_{si}$ with RWG basis functions

$$\mathbf{M}_{si} = \sum_{j=1}^{M_i} m_{ij}\mathbf{S}_{ij} = \{\mathbf{S}_i\}_M^T \bullet \{m_i\}, \quad (22)$$

and then testing integral equation (5) with Galerkin method. Finally, we obtain a matrix equation:

$$[Q]\{u\} + [P]\{m\} = \{V_0\} \quad (23)$$

$\{u\} = \left(\{u_1\}^T, \{u_2\}^T, \ldots \{u_N\}^T \right)^T$, $\{m\} = \left(\{m_1\}^T, \{m_2\}^T, \ldots \{m_N\}^T \right)^T$, and $\{V_0\}$ is the excitation vector for the exterior boundary integral equation.

According to the GIBC in (20) and the expression in (22),

$$\{\mathbf{S}_i\}_M \bullet \{\mathbf{S}_i\}_M^T \bullet \{m_i\} = \{\mathbf{S}_i\}_M \bullet \left[-\hat{n} \times \{\mathbf{N}_i\}^T \right] \bullet \{e_i\} \quad (24)$$

$$\{m_i\} = [G_i]^{-1}[H_i]\{e_i\} = [G_i]^{-1}[H_i][K_i]^{-1}\left(\{V_i\} - [B_i]\{u_i\} \right). \quad (25)$$

where

$$[G_i] = \{\mathbf{S}_i\}_M \bullet \{\mathbf{S}_i\}_M^T \text{ i.e. } [G_i]_{mn} = \int_{S_i} \mathbf{S}_{im} \cdot \mathbf{S}_{in} dS \quad (26)$$

$$[H_i] = \left[\hat{n}_i \times \{\mathbf{S}_i\}_M \right] \bullet \{\mathbf{N}_i\}^T \text{ i.e. } [H_i]_{mn} = \int_{S_i} (\hat{n}_i \times \mathbf{S}_{im}) \cdot \mathbf{N}_{in} dS \quad (27)$$

Consequently,

$$\{m\} = [T]\{u\} + [R]\{b\}, \quad \{b\} = \left(\{V_1\}^T, \{V_2\}^T, \ldots \{V_N\}^T \right)^T \quad (28)$$

Here, $[T]$ and $[R]$ are diagonal block matrices with $[T_i] = -[G_i]^{-1}[H_i][K_i]^{-1}[B_i]$ and $[R_i] = [G_i]^{-1}[H_i][K_i]^{-1}$. Equation (28) provides the matrix expression of the generalized impedance boundary conditions. Notice that, $[T_i]$ and $[R_i]$ are only concerning the structures in domain Ω_i and they have the same expressions for sub-domains with the same components. Thus, for periodic structures, a universal GIBC can be constructed for the unit cell to reduce the memory requirement and set up time.

Finally, we get a full dense matrix equation

$$([Q] + [P][T])\{u\} = \{V_0\} - [P][R]\{b\}. \quad (29)$$

It can be efficiently solved with iteration methods or direct solvers. Because matrices $[G_i]$ and $[K_i]$ are extremely sparse, it is very efficient to invert them by using the sparse matrix direct decomposition provided in software packages such as the multifrontal massively parallel sparse direct solver (MUMPS) [10]. $[H_i]$ and $[B_i]$ are essential sparse matrices. Full dense matrices $[Q]$ and $[P]$ can be transferred to sparse matrices as well by using multilevel fast multipole algorithm. Hence, the memory requirement for storing these sparse matrices is small and the final matrix equation can be solved efficiently. After obtaining $\{u\}$, we can get the magnetic current $\{m\}$ and inner fields $\{e_i\}$, then the exterior field distribution by integral equations (1) and (2).

IV. Numerical Examples

As an application of our numerical method, a RFID tag antenna is modeled and simulated. RFID tag antennas usually work in complex environments, since they are attached to specific objects or put in some packages. To accurately characterize the performance of such antennas, a complete simulation including not only the antenna but also the surrounding objects should be performed. Therefore, an UHF RFID tag antenna embedded in a wooden box is selected as an example. The simulated RFID antenna is a broadband patch antenna which consists of four resonant sub-patches and an inductive feeding loop [11], as shown in Fig. 2(a). This antenna was put in a wooden box, as illustrated in Fig 2(b). The dimension of the box is $350 \times 250 \times 270 mm^3$ and the thickness of each wall is 20 mm. The electrical parameters of Chinese fir are selected in this example, namely, the dielectric constant is 2.67 and the loss tangent is 0.049.

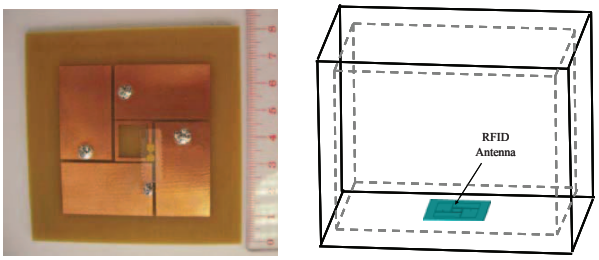

(a) (b)

Figure 2. (a) Prototype of the UHF RFID tag antenna. (b)The RFID antenna is located at the bottom of a wooden box.

First, to demonstrate the accuracy of our model, the input impedance of the isolated antenna without the wooden box is simulated with the proposed FEM-GIBC, which is then

compared with the measurement results. As shown in Fig. 3, the simulated results agree well with the measurements.

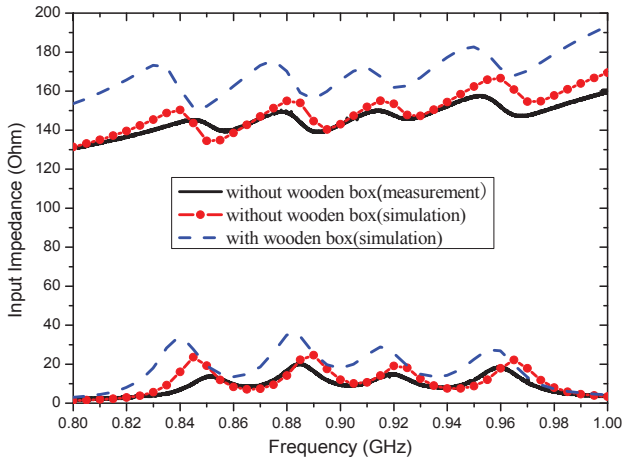

Figure 3. Simulated (dotted line) and measured (solid line) input impedance of the RFID tag antenna. The simulation results when the antenna is put in the wooden box (dashed line) are also shown.

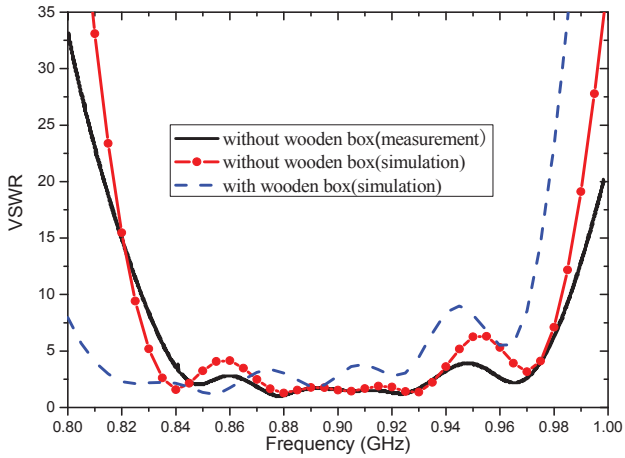

Figure 4. VSWR of the RFID tag antenna, without (solid line) and with (dashed line) the wooden box.

Then, we simulate the case that the antenna is located inside the wooden box. Also shown in Fig. 3, the amplitude of input impedance changes a lot and the resonant peaks of the input impedance shift towards the lower frequencies. These cause significant impedance mismatch between the antenna and the tag chip, as shown in VSWR plotted in Fig. 4. As a result, the power transferred to the chip is reduced and the read range is shorter. The wooden box also distorts the radiation pattern of the antenna (for radiation pattern without wooden box, please refer to [11]), as shown in Fig. 5. The consequence is that the maximum read range direction may not be the boresight any more. All these simulations clearly indicate that the influence of working environment on the actual RFID antenna performance should be carefully taken into account. More numerical examples, including the simulation of finite periodic structures will be presented at the conference.

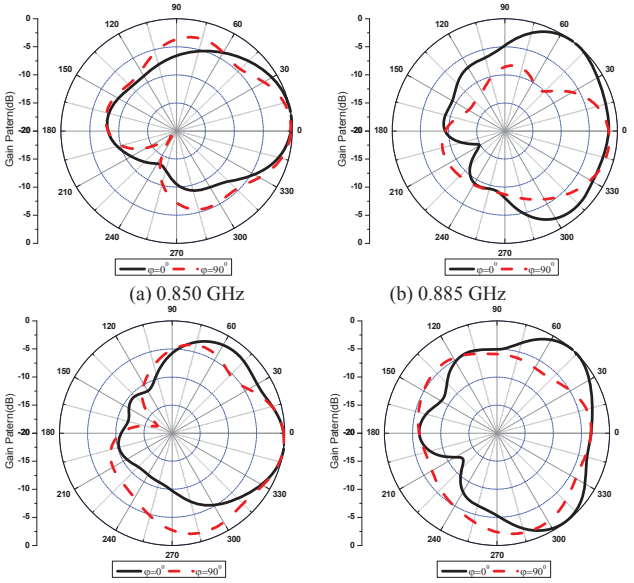

Figure 5. Radiation pattern at (a) 0.85GHz, (b) 0.885GHz, (c) 0.92GHz, and (d) 0.955GHz.

REFERENCES

[1] W. C. Chew, J. M. Jin, E. Michielssen, and J. M. Song, Fast and Efficient Algorithms in Computational Electromagnetics. Boston: Artech House, 2001.

[2] T. B. A. Senior, "Impedance boundary conditions for imperfectly conducting surfaces," Applied Scientific Research, vol. 8, no. 1, pp. 418-436, 1960.

[3] I.-T. Chiang and W. C. Chew, "A coupled PEC-TDS surface integral equation approach for electromagnetic scattering and radiation from composite metallic and thin dielectric objects," IEEE Transactions on Antennas and Propagation, vol. 54, pp. 3511–3516, Nov 2006.

[4] Z. G. Qian, W. C. Chew, and R. Suaya, "Generalized impedance boundary condition for conductor modeling in surface integral equation," IEEE Transactions on Microwave Theory and Techniques, vol. 55, pp. 2354-2364, Nov 2007.

[5] W. C. Chew, Waves and Fields in Inhomogenous Media. Wiley-IEEE Press, 1999.

[6] X. Q. Sheng, J. M. Jin, J. M. Song, W. C. Chew, and C. C. Lu, "Solution of combined-field integral equation using multilevel fast multipole algorithm for scattering by homogeneous bodies," IEEE Transactions on Antennas and Propagation, vol. 46, pp. 1718-1726, Nov 1998.

[7] S. He, W. E. I. Sha, L. Jiang, W. C. Chew, Z. Nie, "Finite element based generalized impedance boundary condition for modeling plasmonic nanostructures," IEEE Transactions on Nanotechnology, unpublished.

[8] J. P. Webb, "Hierarchal vector basis functions of arbitrary order for triangular and tetrahedral finite elements," IEEE Transactions on Antennas and Propagation, vol. 47, pp. 1244-1253, Aug 1999.

[9] S. M. Rao, D. R. Wilton, and A. W. Glisson, "Electromagnetic Scattering by Surfaces of Arbitrary Shape," IEEE Transactions on Antennas and Propagation, vol. 30, pp. 409-418, 1982.

[10] P. R. Amestoy, I. S. Duff, J. Y. L'Excellent, and J. Koster, "A fully asynchronous multifrontal solver using distributed dynamic scheduling," Siam Journal on Matrix Analysis and Applications, vol. 23, pp. 15-41, Apr 2001.

[11] J. Zh. Huang, P. H. Yang, W. C. Chew, T. T. Ye, "A novel broadband patch antenna for universal UHF RFID tags," Microwave and Optical Technology Letters, vol. 52, pp. 2653–2657, Dec 2010.